

# Acoustic and Elastic Anisotropies of Acoustooptic $\text{Ti}_3\text{PSe}_4$ Crystals

Iryna Martynyuk-Lototska<sup>1</sup>, Ivan Roman<sup>2</sup>, Oleksandr Gomonnai<sup>3</sup>, Taras Kryvyy<sup>1</sup>, Oksana Mys<sup>1</sup>, Rostyslav Vlokh<sup>1</sup>

<sup>1</sup> Vlokh Institute of Physical Optics, 23 Dragomanov Street, 79005 Lviv, Ukraine.

<sup>2</sup> Institute of Electronic Physics of National Academy of Sciences of Ukraine, 21 Universytetska Street, 88017 Uzhhorod, Ukraine. vlokh@info.lviv.ua

<sup>3</sup> Uzhgorod National University, 46 Pidhirna Street, 88000 Uzhgorod, Ukraine

## Summary

We report on ultrasonic and elastic properties of acoustooptic (AO)  $\text{Ti}_3\text{PSe}_4$  crystals. Acoustic wave (AW) velocities for different geometries are obtained experimentally, and complete matrices of elastic stiffness and compliance coefficients are computed. Anisotropy of AW propagation is analyzed. The minimal AW velocities are as follows: (i) 1902 m/s for the quasilongitudinal wave propagating at the angle 52 deg with respect to  $a$  axis in  $ab$  plane, (ii) 983 m/s for the quasitransverse wave QT1 propagating in  $cb$  plane along the bisector of  $b$  and  $c$  axes, and (iii) 526 m/s for the quasitransverse wave QT2 propagating along  $a$  (or  $b$ ) axis. The geometries of AO interactions with the slowest acoustic eigenwaves are analyzed. Finally, AO figures of merit  $M_2$  are roughly estimated for the cases of interactions with the slowest AWs. Within isotropic approximation for the elastooptic tensor they are equal to  $\sim 1950 \cdot 10^{-15} \text{ s}^3/\text{kg}$  and  $\sim 2800 \cdot 10^{-15} \text{ s}^3/\text{kg}$  at the isotropic interactions with the slowest quasilongitudinal wave and the slowest AW QT1, respectively. The  $M_2$  parameter as high as  $\sim 18800 \cdot 10^{-15} \text{ s}^3/\text{kg}$  can be expected for the case of anisotropic AO interaction with the slowest AW QT2.

PACS no. 43.35.Cg, 43.35.Sx

## 1. Introduction

$\text{Ti}_3\text{PSe}_4$  belongs to sulfosalt halcogenide compounds that include  $\text{Ti}_3\text{AsSe}_3$ ,  $\text{Ti}_3\text{AsS}_4$ ,  $\text{Ti}_3\text{PSe}_4$ ,  $\text{Ti}_3\text{VS}_4$ ,  $\text{TIGaSe}_2$ ,  $\text{TIGaS}_2$ ,  $\beta\text{-TlInS}_2$  and  $\text{TlInSe}_2$  crystals [1]. Some of these materials are orthorhombic and isomorphic to a known fangite mineral [2]. In particular,  $\text{Ti}_3\text{PSe}_4$  is characterized by the point symmetry group  $mmm$ , with the unit cell parameters equal to  $a = 9.260$ ,  $b = 11.0214$  and  $c = 9.033 \text{ \AA}$  [3]. Its unit cell contains four formula units, and a crystallographic  $b$  axis is perpendicular to a cleavage plane. Note that some well known nonlinear optical materials, which are suitable for the infrared spectral range, belong to the crystalline group of sulfosalt halcogenides [4, 5, 6]. Moreover, they represent efficient Faraday rotators [7, 8]. Besides, the above crystals are among promising acoustooptic (AO) crystals [1, 9, 10].

The main AO parameter is an AO figure of merit (abbreviated as AOFM) defined by the formula  $M_2 = n^6 p_{ef} / \rho v_{ij}^2$ , with  $n$  being the refractive index,  $p_{ef}$  the effective elastooptic coefficient,  $\rho$  the material density and  $v_{ij}$  the velocity of acoustic wave (AW), and  $i$  and  $j$  denoting the directions of acoustic propagation and polar-

ization, respectively. The AOFM determined experimentally for the above materials lies within the range of 100–1370 in the units of AOFM of fused silica, which is equal to  $1.56 \cdot 10^{-15} \text{ s}^3/\text{kg}$  [1, 11] or  $156\text{--}2137 \cdot 10^{-15} \text{ s}^3/\text{kg}$  in the absolute units. Notice that the highest AOFM,  $2137 \cdot 10^{-15} \text{ s}^3/\text{kg}$  is peculiar for the  $\text{Ti}_3\text{PSe}_4$  crystals [1]. Their high AOFM is caused by high enough refractive indices and low AW velocities. Here high refractive indices are a result of strong dispersion, since the absorption edge is located somewhere on the border of visible and infrared ranges, while the AW velocities become low due to softening of the acoustic phonons associated with a pressure induced proper ferroelastic phase transition [3, 12, 13]. In particular, the  $\text{Ti}_3\text{PSe}_4$  and  $\text{Ti}_3\text{AsS}_4$  crystals manifest such transitions at high hydrostatic pressures (1.4 and 2.6 GPa, respectively [12]). Notice that high AO efficiency of sulfosalt halcogenides has caused their wide applications in AO devices, e.g. in tunable proper filters [14] and Bragg cells [15].

In spite of their promising AO characteristics, the properties of these crystals that affect directly the AOFM have not been studied in sufficient detail. In particular, this concerns the anisotropy of AW velocities and the matrices of elastooptic coefficients. Nonetheless, some of these parameters have been investigated in our recent works [16, 17]. For instance, we have found that the  $\text{Ti}_3\text{AsS}_4$  crystals are characterized by rather low velocities  $v_{23}$  and

Received 27 March 2018,  
accepted 13 August 2018.

$v_{32}$  for the transverse AWs, which are equal to 630 m/s. The AOFM has been estimated to be extremely high (approximately  $3 \cdot 10^{-12} \text{ s}^3/\text{kg}$ ) in the case of anisotropic AO interactions with the slowest transverse AWs [16]. A similar situation takes place for the  $\text{Ti}_3\text{AsSe}_3$  and  $\beta$ - $\text{TiInS}_2$  crystals [17, 18]. Note also that knowledge of complete matrices of the elastic stiffness coefficients and the elasto-optic coefficients would enable one to find the optimized geometries of AO interactions, which correspond to the highest AOFMs allowed by the elastic and elasto-optic anisotropies [19, 20].

The present study concerns the  $\text{Ti}_3\text{PSe}_4$  crystals, which seem to be the most efficient AO material among the thallium sulfosalt halcogenides.  $\text{Ti}_3\text{PSe}_4$  is almost optically transparent in the wavelength region 0.85–17  $\mu\text{m}$ , although there are some weak absorption bands between 8 and 17  $\mu\text{m}$  [10]. The principal refractive indices are equal to  $n_a = 2.916$ ,  $n_b = 2.857$  and  $n_c = 2.883$  at the light wavelength 1.15  $\mu\text{m}$  [10]. The crystallographic axis  $b$  represents an acute bisector of the optic axes. The AOFMs of  $\text{Ti}_3\text{PSe}_4$  found at  $\lambda = 1.15 \mu\text{m}$  amount to 515, 1365 and 1370 (in the units of AOFM peculiar to fused silica). These values are associated respectively with the elasto-optic coefficients  $p_{21}$ ,  $p_{22}$  and  $p_{44}$  playing a role of effective elasto-optic coefficients [10].

The experimental data on the AW velocities are still poor. Nonetheless, it is known that they are equal to  $v_{33} = 2200 \text{ m/s}$  and  $v_{11} = v_{22} = 2000 \text{ m/s}$  for quasilongitudinal (QL) waves, whereas the velocities characteristic of quasitransverse (QT) waves are  $v_{1j} = v_{2j} = v_{3j} = 1100 \text{ m/s}$  and  $v_{1j} = v_{3j} = 510 \text{ m/s}$  [1]. The AW attenuation does not exceed 1 dB/ $\mu\text{s}$  at the frequency 100 MHz [1]. Since the experimental results presented above are not enough to comprehend the anisotropy of AO interaction efficiency, in the present work we study experimentally the anisotropy of AW velocities in the  $\text{Ti}_3\text{PSe}_4$  crystals and analyze the anisotropy of their elastic and AO properties.

## 2. Experimental methods and procedures of analysis

$\text{Ti}_3\text{PSe}_4$  crystals were grown using a Bridgman–Stockbarger technique. It follows from the phase diagram of the system  $\text{Ti}_2\text{Se}–\text{P}_2\text{Se}_5$  that the  $\text{Ti}_3\text{PSe}_4$  compound is melted congruently at the temperature  $735 \pm 5 \text{ K}$ . The melt for singlecrystal growth was synthesized in vacuumed quartz ampoules at  $973 \pm 10 \text{ K}$ , using highpurity (99.999%) initial compounds. As a result, single crystals with the diameters 1.5–2.0 cm and the lengths 30–40 cm were obtained. Crystallographic orientation of crystalline boules was performed with an Xray diffraction method. We prepared four nearly cubic shaped samples of  $\text{Ti}_3\text{PSe}_4$  for AW velocity measurements. Their faces were perpendicular to (1)  $a$ ,  $b$  and  $c$  axes, (2)  $a$  axis, and  $[011]$  and  $[11\bar{1}]$  directions, (3)  $b$  axis, and  $[101]$  and  $[10\bar{1}]$  directions, and (4)  $c$  axis, and  $[110]$  and  $[1\bar{1}0]$  directions. The average dimensions of our samples were  $\sim 5 \times 5 \times 5 \text{ mm}^3$ .

The AW velocities were measured with the error not exceeding 2%, using a pulse echooverlap method [21]. We excited the AWs in the samples using standard  $\text{LiNbO}_3$  transducers with the resonance frequency  $f = 10 \text{ MHz}$ , the bandwidth  $\Delta f = 0.1 \text{ MHz}$  and the acoustic power  $P_a = 1–2 \text{ W}$ . The AW velocities were denoted using the indices associated with the crystallographic axes, in a standard notation  $a = 1$ ,  $b = 2$  and  $c = 3$ .

There are nine independent nonzero elastic stiffness coefficients  $C_{klm} = C_{ij}$  for the orthorhombic crystals ( $i, j = 1–6$ , with  $1 = 11$ ,  $2 = 22$ ,  $3 = 33$ ,  $4 = 23$ ,  $5 = 13$ , and  $6 = 12$ ):  $C_{11}$ ,  $C_{22}$ ,  $C_{33}$ ,  $C_{44}$ ,  $C_{55}$ ,  $C_{66}$ ,  $C_{12}$ ,  $C_{13}$ , and  $C_{23}$ . These coefficients can be calculated, following from the known AW velocities and the phenomenological relations

$$\begin{aligned} C_{11} &= \rho v_{11}^2, & C_{22} &= \rho v_{22}^2, & C_{33} &= \rho v_{33}^2, \\ C_{44} &= \rho v_{44}^2, & C_{55} &= \rho v_{55}^2, & C_{66} &= \rho v_{66}^2, \\ C_{12} &= \frac{1}{2} \sqrt{(4\rho v_{66}^2 - C_{11} - C_{22} - 2C_{66})^2 - (C_{11} - C_{22})^2} - C_{66}, \\ C_{13} &= \frac{1}{2} \sqrt{(4\rho v_{55}^2 - C_{11} - C_{33} - 2C_{55})^2 - (C_{11} - C_{33})^2} - C_{55}, \\ C_{23} &= \frac{1}{2} \sqrt{(4\rho v_{44}^2 - C_{33} - C_{22} - 2C_{44})^2 - (C_{22} - C_{33})^2} - C_{44}, \end{aligned} \quad (1)$$

where  $\rho = 6.10 \cdot 10^3 \text{ kg/m}^3$  [10]. The elastic compliances  $S_{km}$  are determined from the matrix of elastic stiffness coefficients  $C_{ij}$  and the formulae [22]

$$\begin{aligned} S_{11} &= (C_{22}C_{33} - C_{23}^2)A^{-1}, \\ S_{22} &= (C_{11}C_{33} - C_{13}^2)A^{-1}, \\ S_{33} &= (C_{22}C_{11} - C_{12}^2)A^{-1}, \\ S_{12} &= (C_{13}C_{23} - C_{12}C_{33})A^{-1}, \\ S_{23} &= (C_{12}C_{13} - C_{11}C_{23})A^{-1}, \\ S_{13} &= (C_{12}C_{23} - C_{22}C_{13})A^{-1}, \\ S_{44} &= 1/C_{44}, \quad S_{55} = 1/C_{55}, \quad S_{66} = 1/C_{66}. \end{aligned} \quad (2)$$

where

$$A = \begin{vmatrix} C_{11} & C_{12} & C_{13} \\ C_{12} & C_{22} & C_{23} \\ C_{13} & C_{23} & C_{33} \end{vmatrix}. \quad (3)$$

The obliquity angle between the acoustic groupvelocity direction and the AW vector can be calculated using the formula [23]

$$\Delta_i = \arctan \frac{1}{v(\phi_i)} \frac{\partial v(\phi_i)}{\partial \phi_i}. \quad (4)$$

Here  $v(\phi_i)$  denotes a function of AW velocity depending upon the angle  $\phi_i$  between the wave vector and the corresponding axis of the crystallographic coordinate system, with the subscript  $i$  referring to the axis perpendicular to the geometric plane under consideration.

The angle of deviation of AW polarization from purely longitudinal type is also a very important characteristic of

AO materials. It has to be properly accounted when deriving phenomenological relations for the effective elastooptic coefficients. We calculated this angle from the Christoffel equation [11] as

$$\zeta_1 = \frac{1}{2} \arctan \frac{(C_{23} + C_{44}) \sin 2\phi_1}{(C_{22} - C_{44}) \cos^2 \phi_1 (C_{44} - C_{33}) \sin^2 \phi_1}, \quad (5)$$

$$\zeta_2 = \frac{1}{2} \arctan \frac{(C_{31} + C_{55}) \sin 2\phi_2}{(C_{55} - C_{11}) \cos^2 \phi_2 (C_{33} - C_{55}) \sin^2 \phi_2}, \quad (6)$$

$$\zeta_3 = \frac{1}{2} \arctan \frac{(C_{11} + C_{66}) \sin 2\phi_3}{(C_{11} - C_{66}) \cos^2 \phi_3 (C_{66} - C_{22}) \sin^2 \phi_3}. \quad (7)$$

The above relations refer respectively to the *bc*, *ac* and *ab* planes. Here  $\phi_1$ ,  $\phi_2$  and  $\phi_3$  are the angles between the AW vector and the *b*, *a* and *a* axes, respectively. The corresponding nonorthogonality of quasitransverse (QT) waves can be calculated in the same manner, with the only difference that the additive factor should be added to the right-hand sides of formulae (5)–(7).

### 3. Results and discussion

AW velocities for the  $\text{TI}_3\text{PSe}_4$  crystals are collected in Table I. The velocities of the QL waves propagating along different spatial directions do not differ essentially. The lowest value,  $v_{66}$ , is equal to  $1926 \pm 26$  m/s, while the highest one to  $v_{11} = 2287 \pm 45$  m/s. The velocities of the QT waves polarized along the *c* (*a*) or *b* (*c*) axes that propagate respectively along the *a* (*c*) or *c* (*b*) directions are rather low ( $\sim 1130$  m/s). Moreover, the velocity of the QT wave, which is polarized along the *a* (*b*) axis and propagates along the *b* (*a*) axis is extremely low ( $v_{12} = v_{21} = 526 \pm 4$  m/s). This value is comparable with that typical for such known AO materials as  $\text{Hg}_2\text{Cl}_2$  (347 m/s) [24],  $\text{TI}_3\text{AsS}_4$  (630 m/s) [16] and  $\beta - \text{TlInS}_2$  (725 m/s) [18]. In general, the velocities of both the QT and QL waves in  $\text{TI}_3\text{PSe}_4$  can be termed as low enough, thus suggesting its efficient applications in various AO devices.

Using the phenomenological relations mentioned above, we have computed complete matrices of the elastic stiffnesses and the compliances. As seen from Table II, the elastic anisotropy with respect to the longitudinal strains is very low, i.e. the elastic stiffness coefficients  $C_{11}$ ,  $C_{22}$  and  $C_{33}$  are almost the same. The same may be said of the elastic compliance coefficients  $S_{11}$ ,  $S_{22}$  and  $S_{33}$ . Notice that the elastic stiffnesses  $C_{66}$  and  $C_{44}$  are the lowest and the elastic compliances  $S_{66}$  and  $S_{44}$  the highest. The reason can be availability of cleavage plane in the  $\text{TI}_3\text{PSe}_4$  crystals, which is perpendicular to the crystallographic *b* axis. In fact, the shear stresses  $\sigma_{12}$  and  $\sigma_{32}$  can lead to large shear strains  $e_{12}$  and  $e_{32}$  and among parallel cleavage planes, due to relatively small van der Waals forces. Notice that a similar situation has earlier been observed for  $\beta - \text{TlInS}_2$  crystals [18].

By solving the Christoffel equation, we have constructed the cross sections of AW velocity surfaces by the principal crystallographic planes. As seen from Figure 1, the QL waves reveal the slowest velocity, 1902 m/s, when

Table I. AW velocities calculated for  $\text{TI}_3\text{PSe}_4$  crystals and for different directions of propagation and polarization.

Directions	Velocity $v_{ij}$ , m/s
[100], [100]	$2287 \pm 45$
[110], [110]	$1926 \pm 26$
[010], [010]	$2052 \pm 8$
[100], [010] or [010], [100]	$526 \pm 4$
[001], [001]	$2105 \pm 23$
[100], [001] or [001], [100]	$1151 \pm 11$
[011], [011]	$2146 \pm 8$
[010], [001] or [001], [010]	$1118 \pm 6$
[101], [101]	$2214 \pm 34$

Table II. Elastic stiffness and compliance coefficients of  $\text{TI}_3\text{PSe}_4$  crystals.

$C_{ij}$ , $10^9$ N/m <sup>2</sup>	$S_{km}$ , $10^{-12}$ m <sup>2</sup> /N
$C_{11} = 31.91 \pm 0.29$	$S_{11} = 43.23 \pm 7.95$
$C_{22} = 25.69 \pm 0.26$	$S_{22} = 59.67 \pm 0.76$
$C_{33} = 27.03 \pm 0.26$	$S_{33} = 59.02 \pm 12.73$
$C_{44} = 7.63 \pm 0.14$	$S_{44} = 131.16 \pm 1.63$
$C_{55} = 8.08 \pm 0.14$	$S_{55} = 123.74 \pm 0.47$
$C_{66} = 1.68 \pm 0.06$	$S_{66} = 562.51 \pm 0.65$
$C_{12} = 12.71 \pm 0.68$	$S_{12} = -12.46 \pm 2.45$
$C_{23} = 14.57 \pm 0.96$	$S_{23} = -25.69 \pm 3.18$
$C_{13} = 14.04 \pm 0.78$	$S_{13} = -15.74 \pm 10.06$

propagating in the *ab* plane at the angle 52 deg with respect to the *a* axis. The QT1 wave is characterized by the slowest velocity 983 m/s, which is peculiar for the propagation direction lying in the *bc* plane (at 45 deg with respect to the *b* or *c* axis). The absolutely slowest AW is QT2, which has the velocity 526 m/s in case of propagation along the *a* or *b* axes.

The QL and QT1 waves manifest weak anisotropy of their velocities. For instance, the velocity of the QT1 wave is almost isotropic for the propagation directions located in the *ac* and *ab* planes. The same is true of the QL wave propagating in the *ac* and *bc* planes. On the other hand, the velocity of the QT2 wave is characterized by higher anisotropy. The velocities of the two QT eigenwaves become the same whenever they propagate along the *c* axis or along the bisectors of the *a* and *b* axes. As a consequence, these directions can be considered as ‘acoustic axes’ for the QT waves.

Now we consider the obliquity of the AW in  $\text{TI}_3\text{PSe}_4$  (see Figure 2). The AW walkoff is an important parameter, which plays a considerable role in the design of AO devices. In particular, this refers to the AO devices that utilize a collinear AO interaction. As seen from Figure 2, the walkoff of the QL wave is not too large. It reaches its largest value,  $-18.4$  deg, in the *ab* plane when the wave vector is directed at 33 deg with respect to the *a* axis. The same is true of the QT1 wave in case if it propagates in the *ab* and *ac* planes. The latter AW manifests larger obliquity angles in the *bc* crystallographic plane. So, the walkoff angles are equal respectively to  $-14.59$  and  $14.29$  deg when

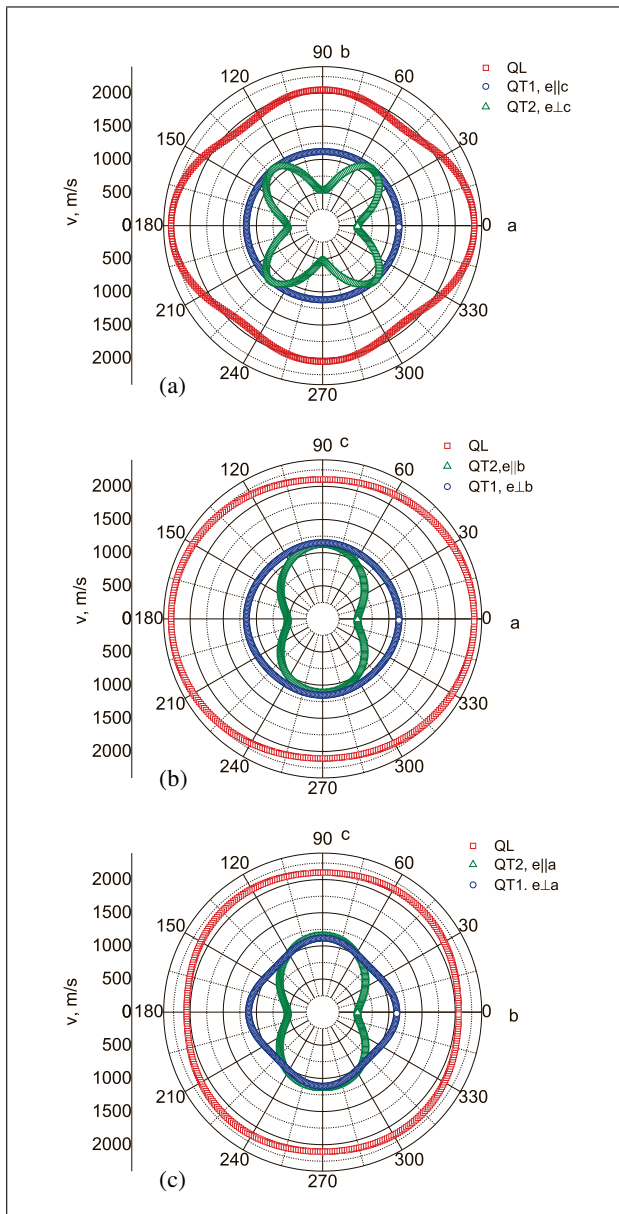


Figure 1. (Colour online) Cross sections of AW velocity surfaces for  $\text{TI}_3\text{PSe}_4$  crystals by the principal crystallographic planes  $ab$  (a),  $ac$  (b) and  $bc$  (c).

the AW vector is inclined by 23 or 66 deg with respect to the  $b$  axis.

The largest walkoff angle is proper for the slowest QT2 wave and the propagation directions lying in the  $ab$  plane. In fact, it reaches 55.77 or  $-58.78$  deg when the AW vector is inclined to the  $a$  axis by 16 or 76 deg. The obliquity angle for this wave propagating in the crystallographic planes  $ac$  and  $bc$  acquires the maximal value of about 40 deg. This angle is equal to zero whenever the AWs propagate along the principal crystallographic directions. Moreover, all of the three eigenwaves have purely transverse or longitudinal polarizations under these conditions. In other words, the angles of deviation from the purely transverse (or longitudinal) polarization states are equal to zero (see Figure 3). The angles of deviation are quite small and do not exceed 5.5 deg in all crystallographic planes for the other

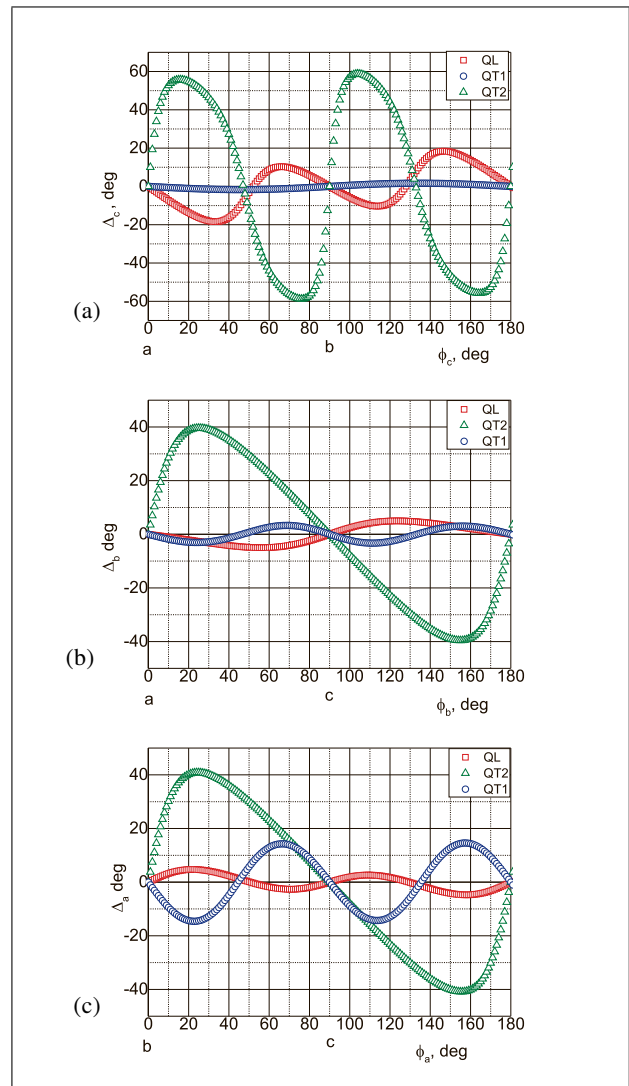


Figure 2. (Colour online) Dependences of obliquity angle (the angle made by the acoustic energy flow and the AW vector) for  $\text{TI}_3\text{PSe}_4$  crystals on the propagation direction of AWs in the crystallographic planes  $ab$  (a),  $ac$  (b) and  $bc$  (c).

directions of propagation of the QL and QT waves (see Figure 3).

Let us now discuss possible geometries of AO interactions with the slowest AWs. It is worthwhile to notice that we can deduce only three of the elasto-optic tensor components from the known AOFM data [1, 10]. Namely, we have  $p_{21} = 0.27$ ,  $p_{22} = 0.44$  and  $p_{44} = 0.17$  (at  $\lambda = 1.15 \mu\text{m}$ ). These tensor components act as effective elasto-optic coefficients in the case of AO interactions with the longitudinal waves termed by their velocities as  $v_{11}$  and  $v_{22}$  and the transverse waves  $v_{32}$  or  $v_{23}$ . However, neither of these waves corresponds to the slowest AW in  $\text{TI}_3\text{PSe}_4$  crystals. Since the complete elasto-optic tensor for  $\text{TI}_3\text{PSe}_4$  is not available in the literature, we use a so-called ‘isotropic approximation’ when estimating the AOFM. Then the approximate equalities  $p_{22} \approx p_{11} \approx p_{33}$ ,  $p_{21} \approx p_{11} \approx p_{23} \approx p_{32} \approx p_{31} \approx p_{13}$ , and  $p_{44} \approx p_{55} \approx p_{66}$  hold true. In fact, this is the approximation in which the structure of elasto-optic tensor is the same as that typical

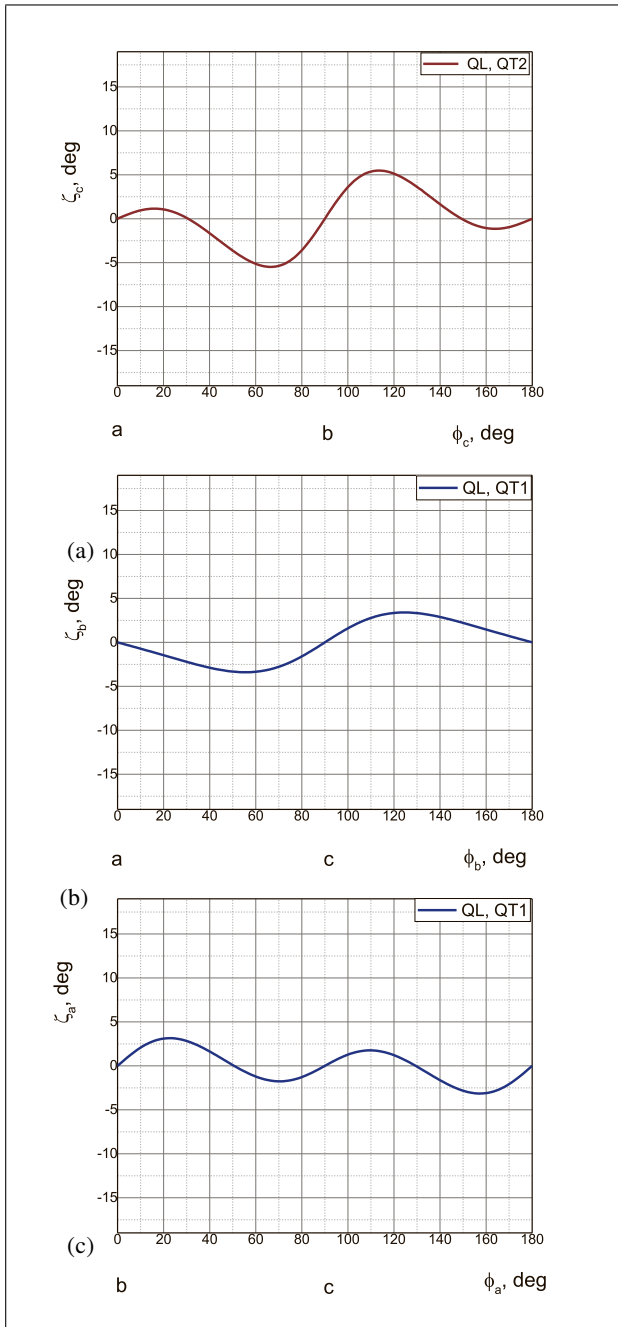


Figure 3. Dependences of the angle of deviation from purely transverse (or longitudinal) polarization states in  $\text{Ti}_3\text{PSe}_4$  crystals on the propagation direction of AWs in the crystallographic planes  $ab$  (a),  $ac$  (b) and  $bc$  (c).

for the highsymmetry isotropic media. Note that the relationship  $p_{44} = (p_{11} - p_{12})/2$  should be valid for the isotropic media, which yields in  $p_{44} = 0.09$ , instead of the value  $p_{44} = 0.17$  obtained experimentally. The difference of above 50% is caused by the fact that, as a matter of fact, we deal with an anisotropic crystalline medium. Nonetheless, the approximation mentioned above enables one to estimate roughly the AOFMs characterizing AO interactions with the slowest acoustic eigenwaves.

Possible types of AO interactions with the slowest AW QL are illustrated in Figure 4a. Here the interaction is

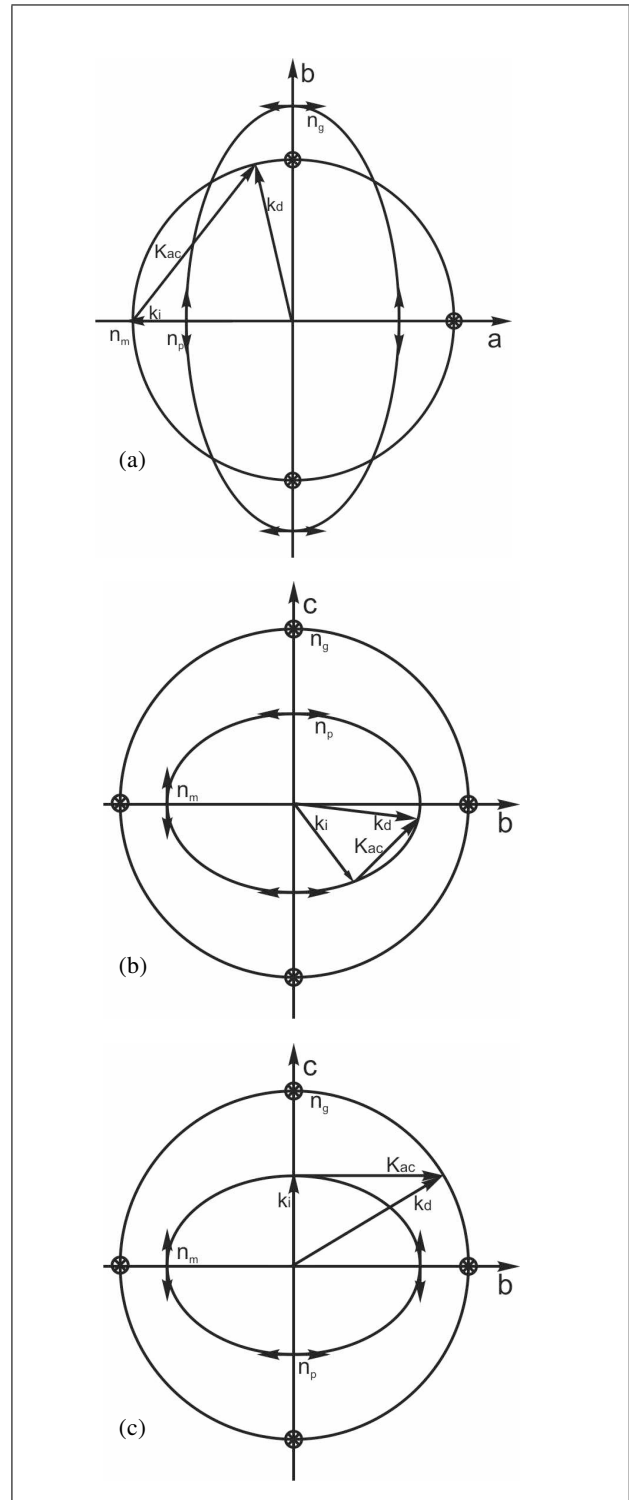


Figure 4. Schematic vector diagrams of AO interactions with the slowest AWs QL (a), QT1 (b) and QT2 (c) in  $\text{Ti}_3\text{PSe}_4$  crystals. Doubleside arrows and crossed circles indicate light polarization directions.  $k_{ac}$ ,  $k_{in}$  and  $k_d$  are wave vectors of the acoustic wave, the incident optical wave and the diffracted optical waves, respectively.

isotropic and corresponds to the case of diffraction of the incident optical wave polarized along the  $c$  axis, with appearance of diffracted Bragg wave polarized along the same axis. The effective elastooptic coefficient for this

diffraction type is equal to  $p_{ef} = p_{31} \cos 52^\circ + p_{32} \sin 52^\circ$  and the AOFM amounts to  $\sim 1950 \cdot 10^{-15} \text{ s}^3/\text{kg}$ . This value is somewhat lower than that obtained experimentally in [10] ( $2137 \cdot 10^{-15} \text{ s}^3/\text{kg}$ ). This can be explained by the fact that, in our particular situation, the contribution of AW slowness to the AOFM is lower than the contribution of large effective elasto-optic coefficient, which is equal to 0.44 in case of the data reported in [10]. Notice also that anisotropic AO interaction in the crystallographic plane  $ab$  cannot be implemented, since the effective elasto-optic coefficients in this case are defined by the  $p_{41}, p_{42}, p_{51}$  and  $p_{52}$  components, which are zero for the orthorhombic crystals.

The isotropic AO interactions with the slow QT1 wave in the crystallographic plane  $cb$  (see Figure 4b) are characterized by the effective elasto-optic coefficient  $p_{ef} = p_{33} - p_{32}$  and a notably higher AOFM,  $\sim 2800 \cdot 10^{-15} \text{ s}^3/\text{kg}$ . In this case the two interacting optical waves, the incident and diffracted ones, are polarized parallel to the  $c$  axis. Again, the anisotropic diffraction in this interaction plane is symmetry forbidden, since we have  $p_{62} = p_{63} = p_{42} = p_{43} = 0$  for the relevant coefficients.

Finally, we consider the AO interaction with the absolutely slowest AW, QT2, that propagates with the velocity 526 m/s in the crystallographic plane  $cb$  (see Figure 4c). In this case the incident optical wave is polarized along the  $b$  axis and the diffracted one along the  $a$  axis. Then the anisotropic diffraction can occur, which involves the slowest QT2 wave. The AW frequency is equal to  $f_a = 485 \text{ MHz}$ . The AOFM for this diffraction type is huge, being roughly equal to  $\sim 18800 \cdot 10^{-15} \text{ s}^3/\text{kg}$ . Probably, this is the highest AOFM value ever expected from solidstate media. Of course, the  $p_{66}$  coefficient can turn out to be lower than  $p_{44}$ . However, even in this case the AOFM can remain extremely high.

#### 4. Conclusions

In the present work we have studied comprehensively the elastic properties of  $\text{Ti}_3\text{PSe}_4$  in order to estimate its AO characteristics. As a result of our AW velocity measurements performed for different geometries, complete matrices of the elastic stiffnesses and the compliances have been obtained. We have found that the  $\text{Ti}_3\text{PSe}_4$  crystals are quite compliant to the mechanical stresses  $\sigma_{12}$  and  $\sigma_{32}$ , which produce the shear strains  $e_{12}$  and  $e_{32}$  in the cleavage planes. Basing on the elastic stiffness tensor, we have constructed the cross sections of the AW velocity surfaces by the principal crystallographic planes. Moreover, the dependences of the walkoff angle and the angle of deviation from purely orthogonal (or longitudinal) AW polarization states on the wave vector direction have been calculated.

We have revealed that the minimal AW velocities are peculiar for the following AWs: (i) the QL wave propagating in the  $ab$  plane at the angle 52 deg with respect to the  $a$  axis (1902 m/s), (ii) the QT1 wave propagating in the  $cb$  plane along the bisector of the  $b$  and  $c$  axes (983 m/s), and (iii) the QT2 wave propagating along the  $a$  (or  $b$ ) axis (526 m/s). We have estimated the AOFM

values peculiar for the AO interactions with these slowest waves. The AOFMs are equal to  $\sim 1950 \cdot 10^{-15} \text{ s}^3/\text{kg}$  and  $\sim 2800 \cdot 10^{-15} \text{ s}^3/\text{kg}$  for the cases of isotropic interactions with the slowest waves QL and QT1, respectively. A gigantic AOFM ( $\sim 18800 \cdot 10^{-15} \text{ s}^3/\text{kg}$ ) can be anticipated for the case of anisotropic Bragg diffraction that involves the QT2 wave. All of the above AO interaction geometries have been analyzed. Finally, we have to notice that AOFM values have been estimated in a rough 'isotropic approximation' for the elasto-optic tensor. Thus, the actual AOFMs can be somewhat different.

#### Acknowledgement

The authors acknowledge financial support of the present study from the Ministry of Education and Science of Ukraine (the Project #0117U000802).

#### References

- [1] M. Gottlieb, T. J. Isaacs, J. D. Feichtner, G. W. Roland: Acoustooptic properties of some chalcogenide crystals. *J. Appl. Phys.* **45** (1974) 5145–5151.
- [2] J. R. Wilson, P. K. Sen Gupta, P. D. Robinson, A. J. Criddle: Fangite,  $\text{Ti}_3\text{AsS}_4$ , a new thallium arsenic sulfosalt from the Mercur Au deposit, Utah, and revised optical data for gillulyite. *Amer. Mineral.* **78** (1993) 1096–1103.
- [3] I. J. Fritz, T. J. Isaacs, M. Gottlieb, B. Morosin: Structure and soft mode behavior of two chalcogenide crystals. *Solid State Commun.* **27** (1978) 535–539.
- [4] J. D. Feichtner, G. W. Roland: Optical properties of a new nonlinear optical material:  $\text{Ti}_3\text{AsSe}_3$ . *Appl. Opt.* **11** (1972) 993–998.
- [5] D. R. Suhre: Efficient second-harmonic generation in  $\text{Ti}_3\text{AsSe}_3$  using focused CO2 laser radiation. *Appl. Phys. B.* **52** (1991) 367–370.
- [6] N. B. Singh, T. Henningsen, Z. K. Kun, K. C. Yoo, R. H. Hopkins, R. Mazelsky: Thallium arsenic selenide crystals for nonlinear optical application. *Prog. Cryst. Growth Character.* **20** (1990) 175–188.
- [7] D. Adamenko, Yu. Vasylykiv, A. Pogodin, O. Kokhan, R. Vlokh: Faraday effect in  $\text{TlInS}_2$  crystals. *Ukr. J. Phys. Opt.* **18** (2017) 197–200.
- [8] D. Adamenko, M. Kushnirivych, O. Kokhan, R. Vlokh: Faraday effect in  $\text{Ti}_3\text{AsS}_4$  crystals. *Ukr. J. Phys. Opt.* **16** (2015) 134–137.
- [9] G. W. Roland, M. Gottlieb, J. D. Feichtner: Optoacoustic properties of thallium arsenic sulphide,  $\text{Ti}_3\text{AsS}_4$ . *Appl. Phys. Lett.* **21** (1972) 52–54.
- [10] T. J. Isaacs, M. Gottlieb, J. D. Feichtner: Optoacoustic properties of thallium phosphorous selenide,  $\text{Ti}_3\text{PSe}_4$ . *Appl. Phys. Lett.* **24** (1974) 107–109.
- [11] V. I. Balakshy, V. N. Parygin, L. E. Chirkov: Physical Principles of Acoustooptics. Radio i Svyaz, Moscow, 1985.
- [12] I. J. Fritz, M. Gottlieb, T. J. Isaacs, B. Morosin: Soft acoustic mode in thallium arsenic sulphide  $\text{Ti}_3\text{AsS}_4$ . *J. Phys. Chem. Solids.* **42** (1981) 269–273.
- [13] R. Vlokh, I. Martynyuk-Lototska: Ferroelastic crystals as effective acoustooptic materials. *Ukr. J. Phys. Opt.* **10** (2009) 89–99.
- [14] M. Gottlieb, Z. Kun: Temporal response of high-resolution acoustooptic tunable filters. *Appl. Opt.* **22** (1983) 2104–2108.

- [15] A. Goutzoulis, M. Gottlieb, K. Davies, Z. Kun: Thallium arsenic sulfide acoustooptic Bragg cells. *Appl. Opt.* **24** (1985) 4183–4188.
- [16] I. Martynyuk-Lototska, M. Kushnirevych, B. Zapeka, O. Krupych, O. Kokhan, A. Pogodin, E. Peresh, O. Mys, R. Vlokh: Acoustic anisotropy of acoustooptic  $\text{Tl}_3\text{AsS}_4$  crystals. *Appl. Opt.* **54** (2015) 1302–1308.
- [17] I. Martynyuk-Lototska, O. Mys, B. Zapeka, A. M. Solomon, O. Kokhan, R. Vlokh: Acoustic, elastic and acoustooptic properties of  $\text{Tl}_3\text{AsSe}_3$  crystals: acoustic isotropic point. *Ukr. J. Phys. Opt.* **16** (2015) 178–186.
- [18] I. Martynyuk-Lototska, I. Trach, O. Kokhan, R. Vlokh: Efficient acousto-optic crystal,  $\text{TlInS}_2$ : acoustic and elastic anisotropy. *Appl. Opt.* **56** (2017) 3179–3184.
- [19] O. Mys, O. Krupych, R. Vlokh: Anisotropy of acoustooptic figure of merit in  $\text{KH}_2\text{PO}_4$  crystals. *Ukr. J. Phys. Opt.* **18** (2017) 83–94.
- [20] O. Mys, O. Krupych, R. Vlokh: Anisotropy of an acoustooptic figure of merit for  $\text{NaBi}(\text{MoO}_4)_2$  crystals. *Appl. Opt.* **55** (2016) 7941–7955.
- [21] E. Papadakis: Ultrasonic phase velocity by the pulse-echo-overlap method incorporating diffraction phase corrections. *J. Acoust. Soc. Amer.* **42** (1967) 1045–1051.
- [22] A. V. Kityk, A. V. Zadorozhna, Ya. Shchur, I. Yu. Martynyuk-Lototska, Ya. Burak, O. G. Vlokh: Elastic properties of  $\text{Cs}_2\text{HgBr}_4$  and  $\text{Cs}_2\text{CdBr}_4$  crystals. *Austr. Journ. Phys.* **51** (1998) 943–957.
- [23] Y. Ohmachi, N. Uchida, N. Niizeki: Acoustic wave propagation in  $\text{TeO}_2$  single crystals. *J. Acoust. Soc. Amer.* **51** (1972) 164–168.
- [24] M. P. Shaskolskaya: *Acoustic Crystals*, Nauka, Moscow, 1982.